OPINION

Proteostasis in complex dendrites

Cyril Hanus and Erin M. Schuman

Abstract | Like all cells, neurons are made of proteins that have characteristic synthesis and degradation profiles. Unlike other cells, however, neurons have a unique multipolar architecture that makes ~10,000 synaptic contacts with other neurons. Both the stability and modifiability of the neuronal proteome are crucial for its information-processing, storage and plastic properties. The cell biological mechanisms that synthesize, modify, deliver and degrade dendritic and synaptic proteins are not well understood but appear to reflect unique solutions adapted to the particular morphology of neurons.

Although it has not been directly measured, the proteome of a single neuron is certainly immense, probably including ~10,000 different types of proteins, with total protein numbers predicted to be in the range of 4×10^{10} molecules per cell[1–3]. The complex morphology of neuronal dendrites and synapses (FIG. 1), with dendrite arbors that encompass ~50,000 µm and ~5,500 µm^3 of length and volume[1,2], respectively, pose unique challenges for the optimization and homeostatic regulation of protein concentration in space and time. In dendrites, the machineries for both protein synthesis and protein degradation are present and have been shown to regulate protein availability during synaptic transmission[4]. In addition, emerging data indicate that proteins exhibit high mobility between synapses[5] and high concentration gradients along the length of the dendrite[6] (FIG. 1b). As such, the minimal compartment that serves as the elementary unit for synaptic plasticity (for example, a synapse, a cluster of synapses, a branchlet, and so on)[7] (FIG. 1) needs to be considered in the context of the distribution of local cell biological machineries.

Although it is probably fair to say that all of the major synaptic molecules have been identified, a dynamic understanding is lacking. Many aspects of local protein synthesis boil down to the question of how limiting resources can be produced and used locally. However, we still know surprisingly little about protein synthesis rates, turnover, mobility and exchange at the scale of the entire neuron. The role and regulation of local protein synthesis and degradation during neuronal development and synaptic plasticity have been reviewed elsewhere[4,8–11]. Here, we discuss emerging dimensions of dendritic and synapse proteostasis and, more specifically, the following three questions. First, how does neuron size affect the partition between somatic and dendritic biosynthetic machineries (FIG. 2a)? Second, what are the spatial scales of subcellular compartmentalization in dendrites (FIG. 2b)? Last, how does this compartmentalization determine the impact of protein synthesis on local membrane composition (FIG. 2c)?

The constraints on cell biology

It has long been recognized that the gigantic size and complexity of neuronal protrusions (FIG. 1a) must exert a colossal pressure on cellular metabolism[12,13]. With surface areas up to 10,000 times larger than those of fibroblasts, neurons probably evolved specialized means to scale up cellular processes, particularly the production, trafficking and turnover of membrane components (FIG. 2a). Indeed, there are many examples of neuron-specific features of common cellular 'machines' in invertebrates and mammals[14–19], which suggests that neurons solved the grand size problem via qualitative changes rather than just scaling up existing solutions. Perhaps consistently, recent attempts to relate brain energy consumption to neuron numbers and morphology across phyla suggest that the scaling up of cortex size during evolution did increase energetic needs but, regardless of neuron size, occurred with a fixed energy budget per neuron[20].

To what extent do neuron size and morphological complexity affect metabolic needs and basic cellular features such as the abundance, distribution and morphology of neuronal organelles? Are there specific cell dimensions above which those relationships show non-linear scaling (FIG. 2a)? These questions remain largely unexplored. During neuronal development, the scaling up of cellular structures with dendritic growth may be possible only up to a certain point. For example, polyribosomes occur every 1 to 2 µm along the lengths of both immature and mature hippocampal dendrites despite an increased density of excitatory synapses in more mature dendrites[21,22]. Differences in the regulation of basic cellular functions also exist between different neuronal types and developmental stages. For example, the morphology of the neuronal Golgi apparatus, one of the main components of the secretory pathway, differs from one neuron type to another, notably among principal excitatory cells of the hippocampus (FIG. 3). It is known that the morphology of the Golgi system directly reflects the specific secretory needs of a cell[23]. It is thus likely that distinct dendritic lengths impose specific demands on secretory functions and thereby affect Golgi morphology[24]. However, the relationship between dendritic length and the morphology of the somatic Golgi is weakly correlated (FIG. 3c), suggesting a more complicated relationship between secretory demands and the organization of secretory organelles (C.H., E.M.S., L. Kochen and S. tom Dieck, unpublished observations). Whether this reflects distinct and neuron-type-specific divisions of membrane protein synthesis at local versus somatic sources remains to be determined.

Similar to many cost–benefit discussions of evolutionary problems, the question of how neuron morphological complexity emerged while preserving cell biological functionality is a chicken and egg problem.

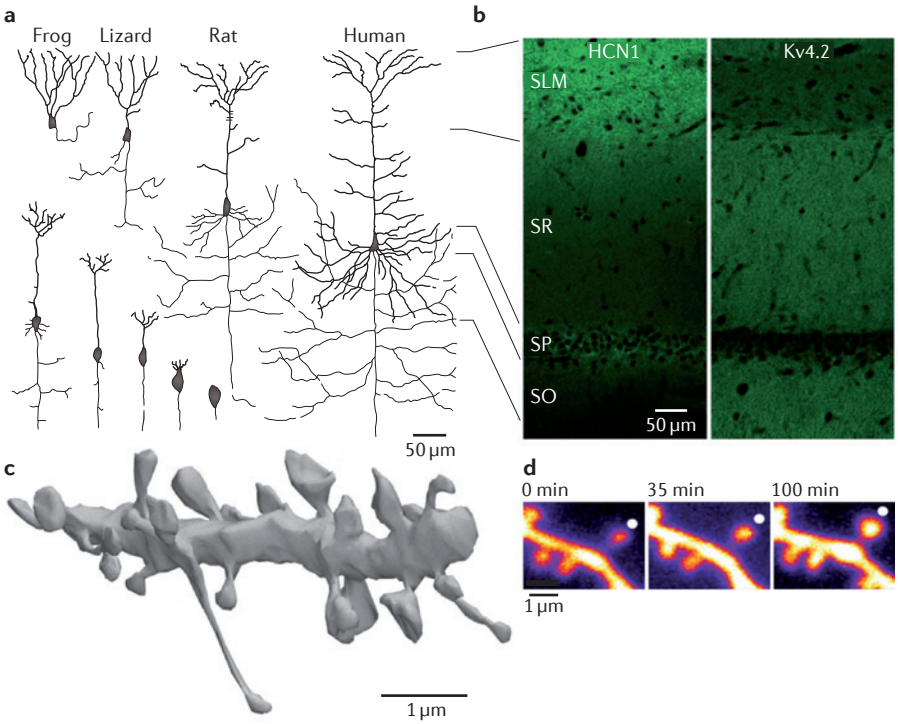

Figure 1 | **Size and compartmentalization of the neuronal membrane.** **a** | Pyramidal cell development in vertebrates. The top panel shows the morphological appearance of principal neurons in the cortex of frogs, lizards, rats and humans. The bottom panel shows the morphology of pyramidal cells at different developmental stages. Note the progressive increase of pyramidal neuron size and morphological complexity (right to left). **b** | Immunolabelling of a hippocampal slice highlights the contrasting distribution of two different potassium channels (hyperpolarization-activated cyclic nucleotide-gated channel 1 (HCN1) and Kv4.2) in the apical dendrites of CA1 pyramidal neurons. Whereas HCN1 is enriched in distal dendrites (upper part of left image), Kv4.2 is more abundant in more proximal segments of dendrites (middle part of right image). The black lines show the correspondence between panels **a** and **b** and indicate the orientation of hippocampal CA1 pyramidal neurons. **c** | Three-dimensional reconstruction of a segment of a CA1 pyramidal neuron apical dendrite, showing the variability of dendritic spine morphology. **d** | Enlargement of a single dendritic spine (white dot) at 0 min, 35 min and 100 min after plasticity induction by focal glutamate uncaging, reflecting the potentiation of an individual synapse. SLM, stratum lacunosum moleculare; SO, stratum oriens; SP, stratum pyramidale; SR, stratum radiatum. Part **a** is adapted from REF. 88 © (1894) C. Reinwald & Cie. Part **b** is adapted, with permission, from REF. 6 © (2012) Elsevier. Part **c** is adapted, with permission, from REF. 41 © (1999) Oxford University Press. Part **d** is adapted, with permission, from REF. 7 © (2011) Elsevier.

On the one hand, the huge dimensions of neurons are a quantitative challenge to which cells seem to have responded by diversifying the functions of existing molecular systems[14–19]. On the other hand (and ignoring, for the moment, dendritic spines), the existence of remote dendritic segments isolated by many bifurcations and situated up to millimetres away from the cell body probably facilitates the compartmentalization of cellular processes (FIG. 2b), 'passively' conferring novel properties to ancient systems. For example, we recently showed that the extensive branching of mature dendrites cumulatively compartmentalizes nascent membrane proteins in the endoplasmic reticulum (ER)[25]. Together with other studies[26,27], these results indicate that although a minimal compartmentalization of secretory trafficking is necessary for asymmetrical dendritic growth and initial dendritic branching, the increasing complexity of more mature dendrites amplifies this very compartmentalization. An interesting possibility is that at a given point in their development, neurons reach a critical size and level of complexity that qualitatively changes their responses to specific constraints or stimuli. The efficient exchange of molecules between the distal dendritic segments and the soma are also affected by dendritic morphology. It is thus likely that the relative impact of global and local protein processing will be different depending on the developmental stage and the neuron type.

Before discussing how these morphological constraints shape resource allocation within neurons, let us first consider the diversity and quantities of synaptic proteins, their local turnover and their site of production within complex neurons.

Synaptic composition and turnover

Diversity of synaptic components and their local turnover. The 10-year period between 1990 and 2000 witnessed an explosion in the identification of the molecular players that populate the synapse. Through advances in biochemistry, molecular biology and the yeast two-hybrid system, the identification and cloning of the major receptors and signalling and scaffolding molecules was accomplished[28]. The number of molecules that mediate and regulate synaptic transmission is large. A recent synthesis of several different proteomic studies identified 2,788 different proteins as integral components of excitatory synapses[29]. In dendritic spines, however, the proteins that are most closely associated with the synapse, physically and functionally, are those that reside in the postsynaptic density (PSD), an electron-dense structure that contains ~300 different protein types, including glutamate receptors as well as scaffolding and signalling molecules[30]. The molecular heterogeneity of individual PSDs has been explored[30,31]. An average PSD in the rat forebrain has a diameter of 360 nm and a mass of 1.1 ±.4 GDa, with stoichiometries of specific proteins ranging from to tens to thousands of molecules (TABLE 1).

Long-term imaging studies *in vivo* indicate that the physical structure of individual synapses can be maintained from days up to months[32,33]. Despite this structural stability, the turnover (the transit of molecules in and out of the synapse) of synaptic proteins within these structures is fast (on the scale of minutes). Over the past decade, advanced live-imaging techniques have revealed the rapid and continuous exchange of synaptic components between synaptic and extrasynaptic compartments[5]. Among these approaches, fluorescence recovery after photobleaching (FRAP) has been particularly useful to compare the synaptic dynamics of various proteins. By bleaching fluorescently tagged synaptic proteins in defined spatial areas, the recovery of fluorescence in the bleached region provides information about both the molecules that remain resident (the 'immobile fraction') as well as those molecules that move into the bleached region (the 'recovered or mobile fraction'). FRAP has, so far, a limited spatial resolution and, because it is a bulk approach, can mask the

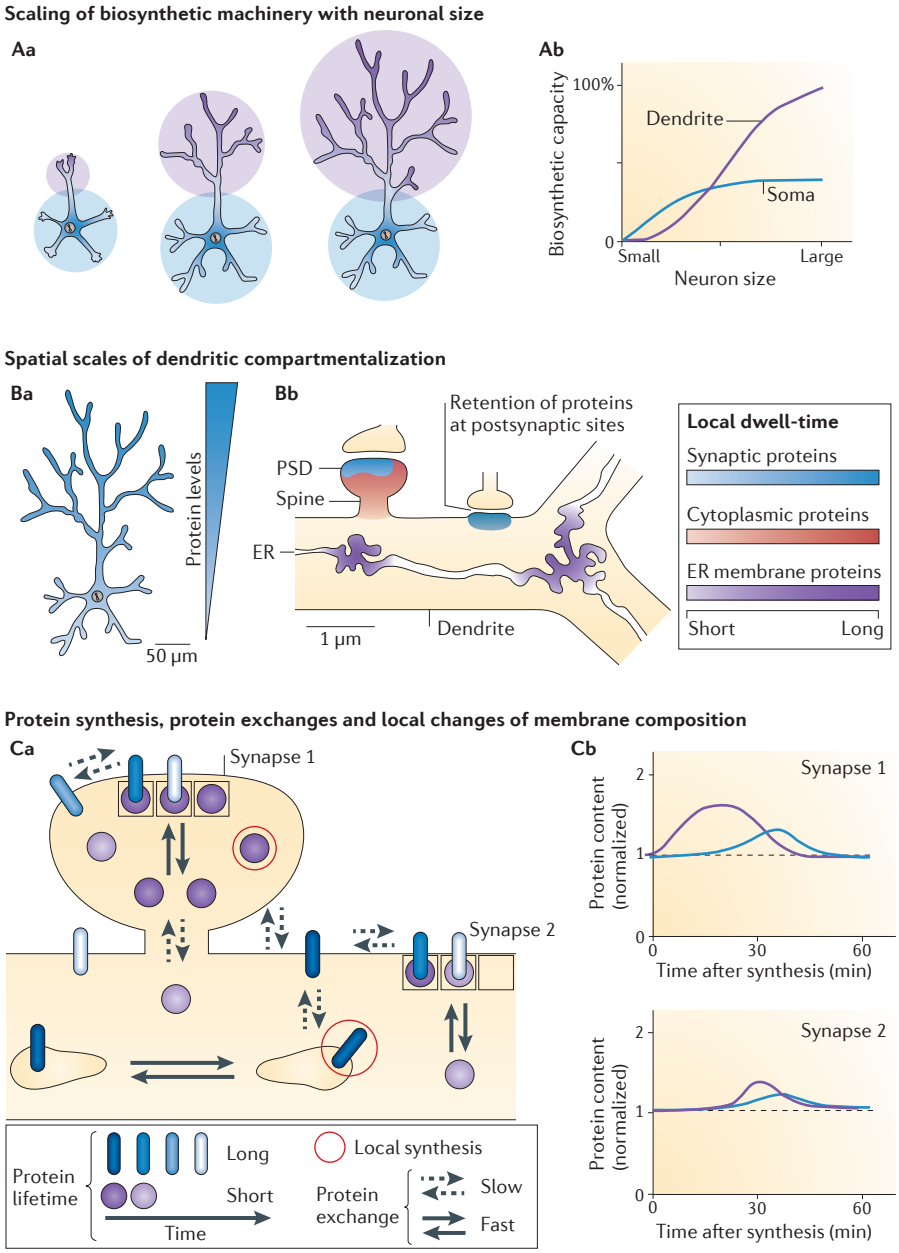

Figure 2 | **Outstanding questions regarding protein synthesis and exchange in complex dendrites.** Hypothetical weights of somatic and dendritic biosynthetic machinery during the development of a pyramidal neuron are represented as bubbles (part **Aa**) or percentage of the maximal biosynthetic capacity (part **Ab**) as a function of neuron size. Distinct spatial scales of proteins compartmentalization in dendrites are shown in part **B**. The protein concentration gradient throughout the apical dendrite of hippocampal pyramidal neurons is shown, in which levels of some proteins (for example, hyperpolarization-activated cyclic nucleotide-gated channel 1 (HCN1)) tend to increase with distance from the soma (part **Ba**). Three examples of subcellular compartmentalization that alter the dwell-time of proteins are shown (part **Bb**): the accumulation and/or retention of synaptic proteins at postsynaptic sites, the passive trapping of cytoplasmic proteins in dendritic spines and the constrained mobility of membrane proteins within the endoplasmic reticulum (ER). Protein turnover, protein lifetime and local changes in membrane composition are shown in part **C**. Local synthesis of two hypothetical proteins in a segment of dendrite in which synapse location, protein stability and turnover at synapses (part **Ca**) affect the variation of their relative levels at synapses over time (part **Cb**). The production of a short-lived protein with a fast synaptic turnover rate (purple circle; the gradual fading of colour represents the transit towards the end of the lifetime of the protein) results in rapid and compartmentalized changes in protein composition in a dendritic spine (synapse 1). By contrast, the synthesis of a more stable membrane protein (blue rod) that has a slower turnover rate in the dendritic shaft results in slower onset and more distributed modifications of synaptic composition (synapse 2). Note that the internalization and recycling of receptors in the dendritic spine are not represented.

complexity of the molecular interactions that structure the synapse[34]. However, the numerous photobleaching studies that are available allow a first glimpse at the apparent turnover of many postsynaptic proteins. As shown in TABLE 1, recovery half-times of the main synaptic proteins vary over an order of magnitude and overall are slower for ion channels than scaffolding proteins (mean ± SEM = 2.8 ± 0.8 min, $n = 7$, for transmembrane proteins ($GABA_A$ receptor subunit γ2 excluded) and mean ± SEM = 1 ± 0.2 min, $n = 11$, for cytoplasmic proteins; $P < 0.05$ using the *t*-test). Similarly, average recovered fractions show that, as a family, synaptic membrane proteins exchange over slower time periods than cytoplasmic proteins in the PSD (mean ± SEM = 39 ± 4% of initial fluorescence, $n = 8$, for membrane proteins and mean ± SEM = 55 ± 6%, $n = 11$, for cytoplasmic proteins; $P < 0.05$ using the *t*-test). As suggested by high-throughput measurements of protein stability (TABLE 2), the lifespan of an average protein is (albeit with huge variability) on the order of a few days. Taken together, this indicates that synaptic proteins cycle in and out of the synapse over many rounds and, as shown by single-molecule imaging[5], explore multiple synapses before being degraded[5]. Although these data provide valuable insights into the timescales over which synaptic composition and properties can be remodelled[34,35], they give little information on how ongoing protein synthesis contributes to the global trading of synaptic components at the scale of the entire neuron. The apparent fast turnover of synaptic components at synapses implies the existence of readily available reserve pools, but strikingly little is known of the nature, replenishment mechanism and local versus global accessibility of these reserve pools (FIG. 2c).

The dendritic transcriptome and the origin of synaptic components. From which source (or sources) are synaptic proteins synthesized? Until recently, the relatively small and largely heterogeneous cast of dendritic and axonal mRNAs that had been identified[36–38] suggested that local protein synthesis is not a major source of synaptic components and may be used only in certain circumstances during synaptic plasticity. The strikingly little overlap between available studies[36–38], however, indicated that only a proportion of the local mRNA population had been identified and prompted us to use more sensitive methods to identify the full complement of mRNAs present in synaptic regions. Through a combination of microdissection, next-generation sequencing, single-mRNA

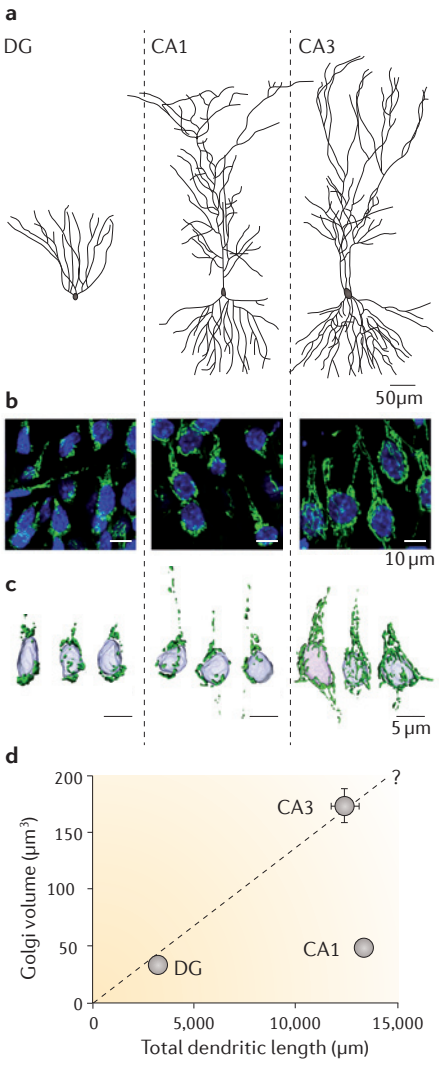

Figure 3 | **Dendritic morphology and the regulation of cellular machinery.** **a** | Semi-schematic morphologies of rat hippocampal principal neurons in dentate gyrus (DG), CA1 and CA3. **b** | Fluorescent images of DG, CA1 and CA3 principal neurons from 4-week-old rats after immunolabelling of the Golgi protein GM130 (also known as GOLGA2) (green). (Nuclei are coloured in blue.) **c** | Three-dimensional reconstructions of the somatic Golgi apparatus in DG, CA1 and CA3 principal neurons, showing the distinct morphologies of the somatic Golgi apparatus (immunolabelling is the same as in part **b**). **d** | Volume of the somatic Golgi (mean ± SEM (n = 10–11 neurons) is taken from two 4-week-old rats) as a function of total dendritic length in the same neuron populations (dendritic lengths were taken from REFS 1,89). Note the non-linearity of Golgi volume increase in neurons with increasing dendritic length and the potentially linear scaling of this parameter in neurons from CA3 and the DG (indicated by the question mark). Part **a** is adapted, with permission, from REF. 90 © (2007) Oxford University Press. Parts **b**–**d** are taken from C.H., E.M.S., L. Kochen and S. tom Dieck, unpublished observations.

counting and high-resolution *in situ* hybridization, we recently identified a surprisingly large number of previously unrecognized mRNAs in the CA1 synaptic neuropile; we obtained a conservative dataset of dendritic and axonal mRNAs (hereafter referred to as the neuropile transcriptome) containing more than 2,500 species[39]. Together with previous studies[40], we estimated that the total transcriptome of a typical CA1 pyramidal neuron contains at least ~5,000 genes, which indicates that a large fraction of its transcriptome can be detected within dendrites[39]. The soma constitutes less than 5% of the somatodendritic volume in a rat CA1 pyramidal neuron[1,41], which implies that the huge majority of the total cellular proteome functions in neurites, a constraint that would explain why mRNA localization seems to be the rule rather than the exception.

Importantly, identified dendritic mRNAs cover diverse classes of proteins and display highly variable expression levels and distinct distribution patterns[39] (FIG. 3d). These include voltage-gated channels, neurotransmitter receptors, synaptic adhesion and scaffolding proteins, signalling molecules as well as components and regulators of the protein synthesis and degradation machinery. More recently, we performed 3′-end deep sequencing[42,43] of neuropile mRNAs (E.M.S., G. Tushev, I. Cajigas and T. Will, unpublished observations) to analyse relative expression levels within the neuropile transcriptome. We found that mRNAs encoding major synaptic proteins (or at least those included in TABLE 1) are, on average, within the top 25% of most abundant species (mean percentile rank ± SEM = 0.75 ± 0.04 for the 25 genes shown in TABLE 1). To use an alternative selection criteria, the 2,285 mRNA species present in our updated neuropile dataset were compared on the basis of their inclusion in relevant gene pathways — 'glutamatergic synapse', 'GABAergic synapse', 'long-term potentiation' and 'long-term depression' — defined in the Kyoto Encyclopedia of Genes and Genomes (KEGG)[44]. This analysis confirmed that mRNAs encoding proteins involved in fast synaptic transmission were particularly abundant within the neuropile transcriptome (mean percentile rank ± SEM = 0.7 ± 0.04 for the 64 genes included in the synaptic subgroup and mean percentile rank ± SEM = 0.5 ± 0.006 for the other 2,221 genes; $P < 10^{-4}$ using the Mann–Whitney U-test). Altogether, these data indicate that many key mediators and regulators of synaptic signalling and dendritic excitability may be produced at a local rather than somatic source.

Local synthesis of ion channels and the organization of the neuronal secretory pathway. Despite differences in the numbers and identity of mRNA species found in neuronal processes, several published studies have identified mRNAs that encode membrane proteins[36–39], raising fundamental questions regarding secretory processing in dendrites. In contrast to cytoplasmic proteins, integral membrane proteins of the cell surface are synthesized, modified and trafficked through the various membrane compartments of the secretory pathway. Although virtually all of the distinct structures that constitute the secretory pathway can be detected in some dendrites[25,45], how and to what extent nascent membrane proteins can be processed and trafficked locally is still a matter of debate. Two features of secretory processing — namely, the apparent continuity of the somatodendritic ER and the microtubule-dependent transport of cargo that is required for sequential processing by the distinct membrane-bound structures of the secretory system[46] — are particularly puzzling, as both could potentially lead to a large spread of proteins produced at a local source (that is, in dendrites), thus compromising local production. Nevertheless, evidence suggests that local membrane protein production can allow for rapid and individual changes in synaptic composition[47–49].

So how have neurons modified the secretory machinery to preserve some degree of specificity for remotely synthesized membrane proteins? We have previously shown that local zones of increased ER complexity compartmentalize ER cargo at dendritic branch points and near dendritic spines, facilitating ER export and local processing at discrete secretory hubs[25]. Although it is not yet clear how membrane cargo transport can be locally restricted

Glossary

Local turnover
The continuous replacement of proteins within a given cellular structure.

Neuropile
Synaptically dense regions of the CNS, containing mostly dendrites, axons and glial cells and a small number of neuron cell bodies.

Secretory pathway
An array of membrane bound structures comprising the endoplasmic reticulum (ER), the ER–Golgi intermediate compartment, the Golgi apparatus, the *trans*-Golgi network and vesiculotubular carriers that synthesizes and processes secreted and membrane proteins of the cell surface.

Table 1 | **Comparison of protein number per PSD, apparent turnover, lifetime and presence of its mRNA in dendrites**

Protein (copy number*)	Apparent turnover‡					Protein half-life			Relative abundance of dendritic mRNA# (gene name)
	Reporter	Assay	$t_{1/2}$ (min)	RF	Refs	PSD *in vitro*§ $t_{1/2}$ (h) (antigen)	Lysate *in vitro*‖ $t_{1/2}$ (days) (gene name)	Total brain *in vivo*¶ $t_{1/2}$ (days) (gene name)	
Integral membrane proteins									
NMDAR GluN1, GluN2A and GluN2B subunits (20)	EPSCs	MK-801	5	30% (20 min)	62	13.5 (GluN1)	1.6 (*Grin1*)		0.5–0.6 (*Grin1*)
	YFP-GluN1	FRAP	6.8	36%	91				
						12.2 (GluN2A)			0.1–0.2 (*Grin2a*)
						15.7 (GluN2B)	1.8 (*Grin2b*)		0–0.1 (*Grin2b*)
AMPAR GluA1, GluA2 and GluA3 subunits (60)	SEP-GluA1	FRAP	3	41%	92			2.1 (*Gria1*)	
	YFP-GluA1	FRAP	2.11	55%	91		1.9 (*Gria2*)	7.2 (*Gria2*)	0.9–1 (*Gria2*)
	SEP-GluA2	FRAP	1.6–3.7	47–53%	93		2 (*Gria3*)	8.1 (*Gria3*)	0.7–0.8 (*Gria3*)
CACNG2 (also known as stargazin)	CACNG2-GFP	FRAP	0.5	25%	94				0.4–0.5 (*Cacng2*)
mGluR1, mGluR5 (20)	mGluR1					4.4 (mGluR1)			
	mGluR5-GFP	FRAP	0.5	54%	95				0.8–0.9 (*Grm5*)
$GABA_AR$	$GABA_AR\ \alpha1^{V257C}$ subunit IPSCs	MTSES	5	70% (30 min)	63				0.8–0.9 (*Gabra1*)
	SEP-$GABA_AR\ \beta3$ subunit	FRAP	2	20%	96				0.9–1 (*Gabrb3*)
	SEP-$GABA_AR\ \gamma2$ subunit	FRAP	0.14	40%	97				0.8–0.9 (*Gabrg2*)
Cytoplasmic proteins									
PSD95 (encoded by *Dlg4*) (300)	PSD95-GFP	FRAP	0.8	20% (4 min)	98	7.5 (PSD95)	3.7 (*Dlg4*)	15.3 (*Dlg4*)	0.9–1 (*Dlg4*)
	PSD95-Venus	FRAP	1	35% (7 min)	99				
	PSD95-YFP	FRAP	4	46%	91				
SHANK1–SHANK3 (150)	GFP-SHANK2	FRAP	2	41% (30 min)	100		4.1 (*Shank2*)		0.9–1 (*Shank1*, *Shank3*)
SAP102 (encoded by *Dlg3*)	GFP-SAP102	FRAP	0.28	80%	101	6.5 (SAP102)	2.1 (*Dlg3*)		0.5–0.6 (*Dlg3*)
SAP97 (encoded by *Dlg1*) (10)	YFP-αSAP97-GFP	FRAP	1.1	40%	102		5 (*Dlg1*)	9.9 (*Dlg1*)	0.5–0.6 (*Dlg1*)
HOMER1–HOMER3 (60)	GFP-HOMER1C	FRAP	1	55% (4 min)	98	2.7 (HOMER)	4.8 (*Homer1*)		0.9–1 (*Homer2*)
SYNGAP (360)									0.8–0.9 (*Syngap1*)
SAPAP1 (also known as GKAP)–SAPAP4 (encoded by *Dlgap1*–*Dlgap4*) (150)	YFP-SAPAP1	FRAP	1	28%	100				0.6–0.8 (*Dlgap3*, *Dlgap4*)
AKAP5 (20)					91	9.2 (AKAP5)			0.6–0.7 (*Akap5*)
CaMKIIα, CaMKIIβ (5,600)	GFP-CaMKIIα	FRAP	2.35	80%	91	20 (CaMKII)	3–3.8 (*Camk2a*, *Camk2b*)	6.5–8.5 (*Camk2a*, *Camk2b*)	0.9–1 (*Camk2a*, *Camk2b*)

Table 1 (cont.) | **Comparison of protein number per PSD, apparent turnover, lifetime and presence of its mRNA in dendrites**

Protein (copy number*)	Apparent turnover‡					Protein half-life			Relative abundance of dendritic mRNA# (gene name)
	Reporter	Assay	$t_{1/2}$ (min)	RF	Refs	PSD *in vitro*§ $t_{1/2}$ (h) (antigen)	Lysate *in vitro*‖ $t_{1/2}$ (days) (gene name)	Total brain *in vivo*¶ $t_{1/2}$ (days) (gene name)	
PP1					91	7.3 (PP1)			0.7–1 (*Ppp1ca*, *Ppp1cb*)
α-actinin 2	α-actinin 2-Venus	FRAP	0.7	60%	99		4.7–6.1 (*Actn1*, *Actn4*)	8.5 (*Actn4*)	0.8–0.9 (*Actn1*)
β-catenin	GFP-β-catenin	FRAP	0.04	60%	103			5 (*Ctnnb1*)	0.8–0.9 (*Ctnnb1*)
Actin	GFP-actin	FRAP	0.4	80%	104			15.3 (*Actb*)	
Gephyrin	Venus-gephyrin (Ge2.6)	FRAP	0.3	50% (10 min)	105				

AKAP5, A-kinase anchor protein 5; AMPAR, AMPA receptor; CACNG2, voltage-dependent calcium channel γ2 subunit; CaMKIIα, calcium/calmodulin-dependent protein kinase II α-subunit; CaMKIIβ, CaMKII β-subunit; *Dlg*, disks large homologue; *Dlgap*; disks large-associated protein; EPSCs, excitatory postsynaptic currents; FRAP, fluorescence recovery after photobleaching; $GABA_AR$, GABA type A receptor; GFP, green fluorescent protein; IPSCs, inhibitory postsynaptic currents; mGluR, metabotropic glutamate receptor; NMDAR, NMDA receptor; PP1, protein phosphatase 1; PSD95, postsynaptic density protein 95; SAP, synapse-associated protein; SAPAP; SAP90/PSD95-associated protein; SEP, super-ecliptic fluorescent protein; SHANK, SH3 and multiple ankyrin repeat domains protein; $t_{1/2}$, half-life or half-time; YFP, yellow fluorescent protein. *Copy numbers per synapse were taken from REF. 28. ‡Apparent turnover half-times and recovery fractions (RFs) at synapses *in vitro*. Indicated values were taken, or approximated by us graphically, from the indicated references. Numbers in brackets after recovered fractions indicate the time at which recovered fractions were quantified when recovery plots did not reach a plateau. §Protein stability half-lives *in vitro* in synaptic biochemical fractions[76]. ‖Protein stability half-lives *in vitro* in total extracts[84]. ¶Protein stability half-lives *in vivo* (total mouse brain)[83]. #Gene name and relative abundance within the neuropile transcriptome indicated by binned percentile ranks (for example, 0.8–0.9 indicates that a given mRNA is within the top 80–90% of most abundant neuropile mRNAs (E.M.S., G. Tushev, I. Cajigas and T. Will, unpublished observations)).

after ER exit and whether local processing requires the presence of Golgi membranes[45,50], these data strongly suggest that neurons have evolved specialized means to locally process membrane and secreted proteins.

The lifetime of synaptic proteins is a critical determinant of how long, how far and at what speed they can be stored and shipped. Although long-lived proteins can potentially be traded over long distances, high shipping costs or slow transportation speed sometimes dictate local production. Analogously, reliance on local production is likely for proteins with a short lifetime and those that cannot be rapidly recruited to a remote location. At present, however, the relative paucity of data on the lifetime of synaptic receptors and other ion channels (TABLE 1) makes it difficult to evaluate the contribution of local membrane protein synthesis to basal synaptic function and dendritic excitability. However, it is clear that the levels of membrane proteins can be locally controlled in a protein synthesis-dependent manner[47], and evidence suggests that some forms of synaptic plasticity require a rapid, and probably local, synthesis of specific receptors. More specifically, two electrophysiological studies have shown that acute (~25 minutes) and specific blockade of AMPA receptor synthesis with small interfering RNA could impair the expression of protein synthesis-dependent forms of synaptic plasticity[48,49]. These results thus indicate that new receptors can be synthesized, assembled and trafficked to synapses within 20–25 minutes in response to exposure to a glutamate receptor agonist[48] or brain-derived neurotrophic factor[49]. For comparison, the complete progression of nascent cargo through the secretory pathway requires up to 120 minutes in specialized secretory cells, such as pancreatic exocrine cells[46]. Many secretory proteins are glycosylated and their sugars are modified as they progress through the secretory pathway[51], a feature that is commonly used to distinguish mature and immature membrane proteins. Indeed, studies in dissociated neurons suggest that nascent AMPA receptors dwell in the secretory pathway for hours[52], challenging the notion that new receptors can be produced over tens of minutes. The reason for this discrepancy is unknown. It is possible, however, that the glycosylation profiles of mature proteins may differ for proteins synthesized in the soma and those produced locally in dendrites. Indeed, the overall low abundance of bona fide Golgi membranes in dendrites[45], suggests that nascent dendritic cargo may 'bypass' specific steps of secretory processing[50] to allow for a more rapid delivery to the cell surface[45]. If this is the case, then one expects that ion channels and other membrane proteins will possess distinct functional properties when synthesized in the soma or in dendrites. This remains to be determined.

Protein exchanges in the dendrite

It is now quite clear that, at least in dendritic spines, the local control of membrane trafficking is a key mechanism to control the level of postsynaptic neurotransmitter receptors[53,54]. However, we still do not know much about the extent to which local intracellular reservoirs exchange cargo with other pools of receptors (for example, shaft endosomes, the extrasynaptic membrane, and so on) (FIG. 2c). In addition, whereas the dynamics of receptors are now better understood at the scale of the individual synapse[5], little is known about receptor exchanges over larger spatial scales. The rate of these global exchanges must be different for proteins freely diffusing in the cytoplasm, those in cellular membranes or those actively transported in tubulovesicular structures along microtubules. Owing to the saltatory nature of kinesin- or dynein-mediated transport[55], it is easy to envision how microtubule-based transport could be controlled to prevent (or enable) cargo exchange and deposition over long distances. For example, phosphorylation of a kinesin family member by calcium/calmodulin-dependent protein kinase II (CaMKII) results in the release of cargo[56]. As synaptic activity controls CaMKII activity[57], this could provide a mechanism by which synaptic activity terminates dendritic tubulovesicular trafficking, resulting in the local release of cargo at activated synapses. Importantly, long-range

Table 2 | **High-throughput measurements of global protein stability**

Model (tissue or cell type)	Method	Protein turnover half-life ($t_{1/2}$)				Refs
		Median	Range	Mean ± SEM	*n* (proteins)	
in vitro						
Yeast	Metabolic labelling and MS	34.25 h	(0*) 7.6–217 h	32.3 ± 3.3 h	52	106
Yeast‡	Tagged-protein library and immunoblotting	43 min		43 min	3,751	107
Human lung cancer cells	Metabolic labelling and MS	20.4 h	Min–months	8.5 h	576	108
Human lung cancer cells	Tagged-protein library and photobleaching		45 min–22.5 h	9 h	100	109
Human cervical cancer cells§	Metabolic labelling and MS	35.5 h	8.1 h–5 months	40.5 ± 1 h	4,106	110
Mouse myoblasts§	Metabolic labelling and MS	43.2 h	10.5 h–18 months	68.6 ± 1 h	3,528	110
Cultured neurons (total proteins)	Metabolic labelling and MS	4.2 days		5.1 days	2,802	84
Cultured neurons (synaptic proteins)	Metabolic labelling and MS	3.7 days		4.1 days	191	84
in vivo						
Mouse (brain, liver and blood)	Metabolic labelling and MS		0.17 min–11.5 months		1,716	83
Mouse (brain)	Metabolic labelling and MS	9 days			1,010	83
Mouse (liver)	Metabolic labelling and MS	3.5 days			1,122	83
Mouse (blood)	Metabolic labelling and MS	3 days			334	83
Mouse (liver)	Metabolic labelling and MS	4.2 days	14.4 h–9.8 days	4.1 ± 0.3 days	31	111
Mouse (kidney)	Metabolic labelling and MS	4.4 days	1.4 –12.4 days	4.9 ± 0.4 days	32	111
Mouse (cardiac muscle)	Metabolic labelling and MS	10.5 days	3.1 days–7.7 months	22.4 ± 7.6 days	30	111
Mouse (skeletal muscle)	Metabolic labelling and MS	28.3 days	3–53.3 days	27.3 ± 3.2 days	20	111

MS, mass spectrometry. *Zero decay after correction for protein dilution due to cell growth over a 51-hour time course. ‡Protein synthesis was inhibited during the experiment. §Non-dividing cells.

exchanges throughout dendrites also seem to be limited for proteins diffusing in continuous structures such as the cytoplasm[58], the ER[25] and the plasma membrane[59]. An interesting notion is that dendritic spines and PSDs act as diffusion sinks and traps that — passively or by actual binding — limit the exploration of large areas of dendritic terrain[59] (FIG. 2c). Consistently, and in contrast to local membrane trafficking, the long-range diffusion of receptors at the cell surface seems to make only a minor contribution to the fast turnover of relatively distal synapses[60] (but see REF. 61). Although the entire extrasynaptic plasma membrane contains an enormous reserve pool of synaptic receptors[62–64], the relatively slow mobility of membrane proteins[5] and the overall complexity of the dendritic surface probably limit the actual availability of nascent proteins at the dendritic surface. Consistently, recent work suggests that anomalous diffusion within the ER restricts the dendritic volume explored by nascent membrane proteins before ER exit[25]. Altogether, these data indicate that there can be substantial differences between local protein mobility and the global exchange at the scale of the entire neuron, and perhaps suggest that the total levels of these proteins may not necessarily predict their local availability. In other words, a local production of relatively long-lived components in some instances may be required to maintain a reliable supply.

Resource allocation in dendrites

The discovery of the rapid recruitment or loss of proteins, such as AMPA receptors, during long-term potentiation (LTP) and long-term depression (LTD) of excitatory synapses[53,65–68] has proven to be a valuable experimental paradigm for understanding how basic cellular processes contribute to the control of synaptic properties. The regulation of protein exchanges between the postsynapse, the plasma membrane and intracellular pools has emerged as a critical factor that tunes synaptic strength and dendritic excitability[54,69]. However, it is unclear what fraction of a specific protein is actually in use at any given time and whether these fractions are different for distinct types of proteins.

Despite various shapes and functional properties, synapses display invariant features, resulting, for example, in a strong correlation between the number of available synaptic vesicles and the number of postsynaptic receptors or the PSD area[70,71]. Exploiting such correlations to study ultrastructural changes occurring during synaptic potentiation, recent experiments showed that despite striking variations of synapse size and density, total excitatory and inhibitory PSD areas per unit of dendritic length are unchanged in activated dendrites[72]. This strongly indicates that plasticity induction may require redistribution of limited resources that are 'shared' between synapses (FIG. 2c). Consistent with this idea, imaging of PSD95 (also known as DLG4) dynamics *in vivo* showed that neighbouring synapses locally compete for available molecules that are estimated to constitute ~1% of the total protein content at the scale of the entire cell[73]. As suggested by the observation that overexpression of PSD95 can lead to increased synapse strength and size[74], the basal levels of the endogenous protein seem

to be limiting. It is thus tempting to speculate that the wealth of activity-dependent mechanisms that facilitate PSD95 recruitment at synapses[75] may lead to an abrupt and local depletion of available resources. The high abundance of *Psd95* mRNAs among dendritic RNAs suggests an important local synthesis of the protein[4] (TABLE 1), which would thus be crucial for maintaining the local availability of this otherwise relatively stable[76,77] and abundant protein.

Global versus local protein lifetimes

Measurements of apparent protein stability in PSD fractions revealed half-lives, ranging from minutes up to tens of hours[76] (TABLE 1). If it is pretty clear why and how cytoplasmic proteins with short lifetimes might be locally synthesized at synapses[78] (FIG. 2c), the case of surface ion channels is more problematic. As receptor dwell-times at synapses and internalization rates are on the order of seconds and minutes, respectively[5,79,80], receptors undergo many rounds of internalization and recycling before being degraded, a process that is likely to be all the more efficient in dendritic spines[54]. This relatively fast recycling process may allow a local concentration of receptors taken from a diffuse pool, perhaps obviating the need for local synthesis. Conversely, the activity-dependent targeting of internalized receptors for lysosomal degradation[79] and the activity-dependent recruitment of the proteasome in dendritic spines[81] suggest that synaptic protein lifetime is subject to potent and compartment-specific regulations[76,82]. Indeed, compared with average protein half-lives measured in bacteria, fibroblasts or total cultured neuron extracts[83,84] (TABLES 1,2), values obtained from isolated synaptic fractions suggest that synaptic proteins have a fast turnover (mean half-life ± SEM = 3.3 ± 0.5 hours for global radioactivity loss after metabolic labelling, $n = 6$ experiments, and mean half-life ± SEM = 9 ± 3 hours for the 10 proteins for which it has specifically been measured; see REF. 76 and TABLE 1). More specifically, measurements of the half-life of PSD95 in total neuronal extracts (~36–87 hours)[77,84] and synaptic fractions (~7 hours)[76] revealed sensible differences between the global and local stability of this synaptic protein.

Interestingly, data suggest that the polyubiquitylation and degradation of a few 'master' scaffolding proteins such as SAP90/PSD95-associated protein 1 (SAPAP1; also known as GKAP and DLGAP1) and SH3 and multiple ankyrin repeat domains protein (SHANK) by the proteasome leads to the co-depletion of other synaptic molecules (for example, GluN2B) that are not thought to be targeted by the proteasome[76]. Although it is not yet clear whether these proteins are locally degraded or simply relocalized to extrasynaptic pools, these results suggest that synaptic proteins live 'in the fast lane' and may have a shortened lifetime. Consistent with this idea, the maintenance of dendritic structure seems to require ongoing secretory trafficking[26], indicating that key membrane or secreted proteins need to be replaced within hours. Combined with the overall low mobility of integral membrane proteins at the scale of an entire dendrite, variations of their stability in space and time may be such that an acute and local synthesis of ion channels may be necessary. Similarly, and as discussed above for PSD95, the efficient sequestration of available cytoplasmic proteins, as well as the rapid and input-specific variations of available binding slots and the local competition between synapses, may result in the local depletion of available molecules and may thus require local synthesis.

PrP products and synaptic tagging

It is commonly believed that although changes in the phosphorylation status of receptors and associated molecules and their local trafficking can drive plasticity of post-synaptic responses over the course of minutes[53,54], longer lasting changes in synaptic strength requires the activation of transcriptional programmes and/or *de novo* protein synthesis[4]. A common view is that the resulting 'plasticity-related protein' (PrP) products are released in a shared pool but only incorporated in those synapses that have been tagged by (during) their prior potentiation[85], explaining how resources produced remotely can be locally incorporated in an input-specific manner. The actual availability of this common pool, the identity and distinctness of PrP products remain unknown. A recent paper described elegant approaches to tackle these questions. By combining focal glutamate uncaging and pharmacological activation of protein kinase A, Govindarajan *et al.*[7] controlled the induction of 'early' or 'late' forms of LTP (E-LTP and L-LTP, respectively) at individual synapses (FIG. 4a). Consistent with the original formulation of the synaptic tagging and capture model[85], the authors showed that PrP products produced in response to L-LTP induction and recruited at activated synapses can also be recruited by nearby synapses previously or subsequently tagged by E-LTP induction, converting E-LTP to L-LTP at tagged synapses[7] (FIG. 4b). Taking advantage of this temporal bidirectionality and the synthesis-dependent or synthesis-independent nature of PrP products and the synaptic tag, the authors selectively measured the half-lives of these components (~90 minutes for PrP products and ~120 minutes for the tag). By monitoring L-LTP and E-LTP-to-L-LTP conversion in synapse pairs located on the same or distinct dendritic branches, they found that the propagation of PrP products was limited by branch points (FIG. 4c), providing a compelling illustration of the influence of cellular morphology on resource sharing in elaborate dendrites. By focusing on specific forms of synaptic plasticity that rely on *de novo* synthesis of cytoplasmic[78] versus membrane proteins[48,49], it should be now possible to provide a more complete picture of how these temporal and morphological constraints shape resource allocation throughout dendrites. In the long run, it will be interesting to determine how differences in protein mobility and stability, specific dendritic morphologies and the partition between somatic and dendritic protein synthesis determine how fast, for how long and to what extent synaptic properties can be adjusted in an input-specific manner.

Concluding remarks

Although it is now well established that various forms of synaptic plasticity require *de novo* protein synthesis[4], the identity of the proteins that are being synthesized still has to be determined. Conversely, evidence suggests that activity-dependent protein degradation is also tightly controlled during synaptic plasticity[76,81]. However, plasticity-related 'degromes' have not been characterized. Future characterization of both the plasticity-related proteome and degrome must be quantitative, as it is likely that the major plasticity-related changes will be in the relative stoichiometries rather than identities of synaptic proteins. Although the standard experimental method to establish the protein synthesis- and degradation-dependence of a given biological response is still through the use of generic inhibitors of the translation and degradation machineries, the development and availability of experimental means to selectively inhibit the synthesis of specific proteins and trigger or block their degradation is important.

As illustrated by TABLE 1, there is growing information but limited consensus on the global turnover of synaptic proteins and dendritic ion channels (to say nothing about mRNA processing and translation) to start mining for probable links between these parameters. Although available data suggest important discrepancies between protein

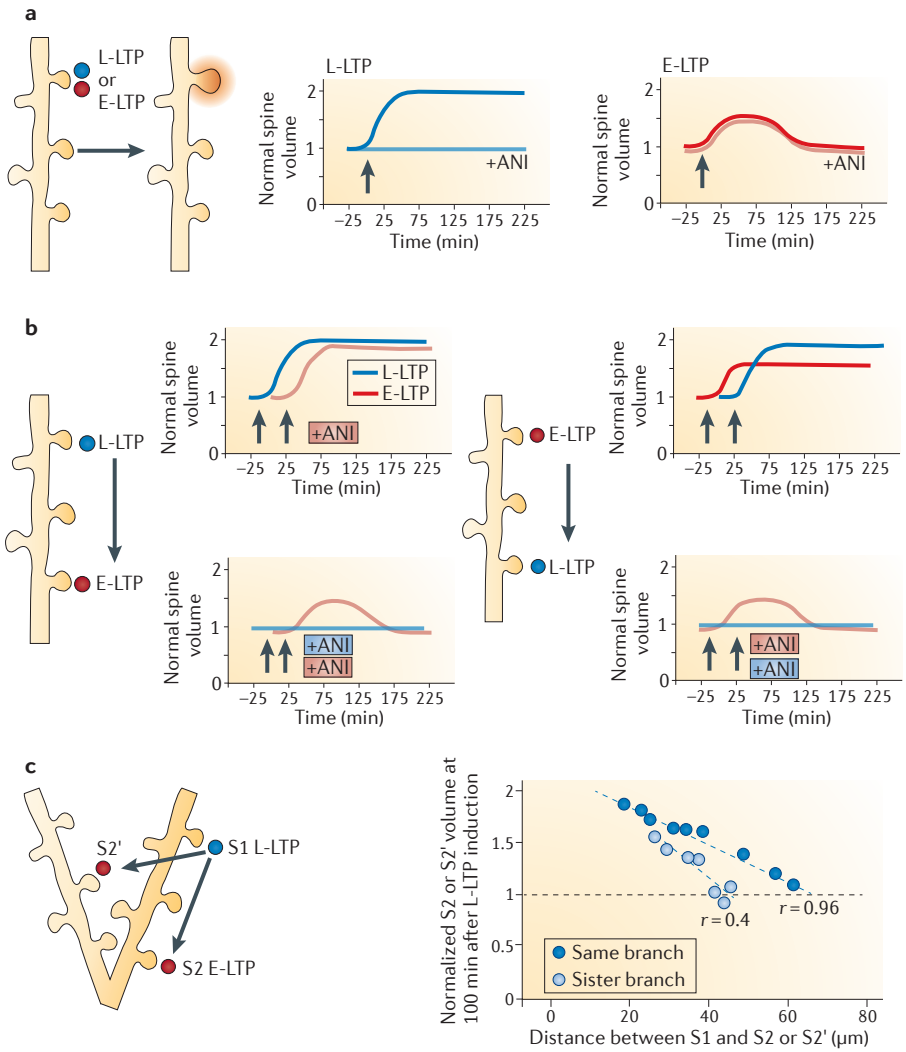

Figure 4 | **Synaptic competition and resource allocation in dendrites. a** | Early long-term potentiation (E-LTP; red circle) and late LTP (L-LTP; blue circle) and the resulting spine enlargement (red shading around spine; left panel) can be induced by focal glutamate uncaging at individual synapses (indicated by arrows in the graphs), and their contrasting reliance on protein synthesis is shown by exposure to the translation inhibitor anisomycin (ANI) (middle and right panels). Whereas L-LTP induction results in a long-lasting increase in spine volume (middle panel, dark blue trace) that is completely abolished by protein synthesis inhibitors (light blue trace), E-LTP induction results in a more transient spine enlargement (right panel, dark red trace) that is not affected by ANI (light red trace). **b** | Synapse tagging and capture in pairs of spines activated by L-LTP ('donor' synapse) or E-LTP ('acceptor' synapse) is demonstrated by the conversion of E-LTP to L-LTP at 'tagged' synapses stimulated after L-LTP induction (left scheme) or before L-LTP induction (right scheme). In the left scheme, top graph, the conversion of E-LTP to L-LTP (shown by the lack of decay in the E-LTP trace) is not blocked by ANI and thus relies on the recruitment of proteins (synaptic tags) induced after prior L-LTP induction. By contrast, ANI added concurrently with the L-LTP induction protocol prevents L-LTP expression at both synapses, but E-LTP induction is unaffected (bottom graph). In the right scheme, induction of E-LTP followed by L-LTP induction at a neighbouring synapse allows the conversion of E-LTP to L-LTP (indicated by lack of decay of the red trace in the top graph). Application of ANI concurrently with E-LTP induction results in the usual E-LTP formation and decay profile (bottom graph, red trace), indicating that it has not been converted to L-LTP. ANI applied concurrently with the L-LTP induction protocol results in a complete block of spine volume changes (bottom graph) . **c** | The experiment described in part **b**, in which prior L-LTP induction allows E-LTP-to-L-LTP conversion in tagged synapses, is used here to test the distance of propagation of the plasticity-related protein products (synaptic tags) in synapse pairs at varying distances in the same (S2) or sister (S2') dendritic branches. The graph on the right shows that the propagation of synaptic tag proteins is reduced in a sister branch compared with the same branch, and illustrates how dendritic branch points restrict the distribution of these proteins. Figure is adapted, with permission, from REF. 7 © (2011) Elsevier.

stability measurements taken from cultured cells and *in vivo* by mass spectrometry after metabolic labelling (TABLE 2), it is not yet clear to what extent these differences are real or owing to differences in technique. Indeed, important differences may exist in the overall accessibility and recycling of labelled precursors in distinct organs and cell populations *in vivo*, which complicates the interpretations of available results. Importantly, the contribution of local ongoing protein synthesis to dendritic protein homeostasis and hence synaptic properties and dendritic excitability and its deregulation in pathological contexts is most likely to be different in distinct neuronal types and specific compartments (for example, dendritic spines). It is thus now critical to develop appropriate tools to selectively label, detect and purify mRNA and proteins in targeted cell populations and cell compartments in normal and pathological brains. Although experimental strategies to label RNAs[86] and proteins[87] in a genetically restricted manner exist and have been characterized in cultured cells, efforts should now be made to generate and characterize genetically modified models to use these molecular tools *in vivo*.

Cyril Hanus and Erin M. Schuman are at The Max Planck Institute for Brain Research, Max von Laue Strasse 4, 60438 Frankfurt, Germany.

Correspondence to E.M.S.
e-mail: erin.schuman@brain.mpg.de

doi:10.1038/nrn3546
Published online 31 July 2013

1. Ishizuka, N., Cowan, W. M. & Amaral, D. G. A quantitative analysis of the dendritic organization of pyramidal cells in the rat hippocampus. *J. Comp. Neurol.* **362**, 17–45 (1995).
2. Ascoli, G. A., Donohue, D. E. & Halavi, M. NeuroMorpho.Org: a central resource for neuronal morphologies. *J. Neurosci.* **27**, 9247–9251 (2007).
3. Moran, U., Phillips, R. & Milo, R. SnapShot: key numbers in biology. *Cell* **141**, 1262–1262.e1 (2010).
4. Cajigas, I. J., Will, T. & Schuman, E. M. Protein homeostasis and synaptic plasticity. *EMBO J.* **29**, 2746–2752 (2010).
5. Triller, A. & Choquet, D. Surface trafficking of receptors between synaptic and extrasynaptic membranes: and yet they do move! *Trends Neurosci.* **28**, 133–139 (2005).
6. Nusser, Z. Differential subcellular distribution of ion channels and the diversity of neuronal function. *Curr. Opin. Neurobiol.* **22**, 366–371 (2012).
7. Govindarajan, A., Israely, I., Huang, S. Y. & Tonegawa, S. The dendritic branch is the preferred integrative unit for protein synthesis-dependent LTP. *Neuron* **69**, 132–146 (2011).
8. Bassell, G. J. & Warren, S. T. Fragile X syndrome: loss of local mRNA regulation alters synaptic development and function. *Neuron* **60**, 201–214 (2008).
9. Vo, N. K., Cambronne, X. A. & Goodman, R. H. MicroRNA pathways in neural development and plasticity. *Curr. Opin. Neurobiol.* **20**, 457–465 (2010).
10. Lin, A. C. & Holt, C. E. Local translation and directional steering in axons. *EMBO J.* **26**, 3729–3736 (2007).
11. Mabb, A. M. & Ehlers, M. D. Ubiquitination in postsynaptic function and plasticity. *Annu. Rev. Cell Dev. Biol.* **26**, 179–210 (2010).
12. Golgi, C. *Sulla Struttura Delle Fibre Nervose Midollate Periferiche e Centrali, Ricerche del C. Golgi, Lette al R. Istituto Lombardo Nell' Adunanza del Dicembre 18 Dicembre 1879* (Milano, 1880) (in Italian).

13. Ramón y Cajal, S. *Histologie du Système Nerveux de l'Homme & des Vertébrés* (A. Maloine, 1909) (in French).
14. Kuo, C. T., Zhu, S., Younger, S., Jan, L. Y. & Jan, Y. N. Identification of E2/E3 ubiquitinating enzymes and caspase activity regulating *Drosophila* sensory neuron dendrite pruning. *Neuron* **51**, 283–290 (2006).
15. Kim, A. H. *et al.* A centrosomal Cdc20–APC pathway controls dendrite morphogenesis in postmitotic neurons. *Cell* **136**, 322–336 (2009).
16. Huang, Z., Zang, K. & Reichardt, L. F. The origin recognition core complex regulates dendrite and spine development in postmitotic neurons. *J. Cell Biol.* **170**, 527–535 (2005).
17. Baas, P. W., Deitch, J. S., Black, M. M. & Banker, G. A. Polarity orientation of microtubules in hippocampal neurons: uniformity in the axon and nonuniformity in the dendrite. *Proc. Natl Acad. Sci. USA* **85**, 8335–8339 (1988).
18. Stiess, M. *et al.* Axon extension occurs independently of centrosomal microtubule nucleation. *Science* **327**, 704–707 (2010).
19. Lin, S., Liu, M., Mozgova, O. I., Yu, W. & Baas, P. W. Mitotic motors coregulate microtubule patterns in axons and dendrites. *J. Neurosci.* **32**, 14033–14049 (2012).
20. Herculano-Houzel, S. Scaling of brain metabolism with a fixed energy budget per neuron: implications for neuronal activity, plasticity and evolution. *PLoS ONE* **6**, e17514 (2011).
21. Ostroff, L. E., Fiala, J. C., Allwardt, B. & Harris, K. M. Polyribosomes redistribute from dendritic shafts into spines with enlarged synapses during LTP in developing rat hippocampal slices. *Neuron* **35**, 535–545 (2002).
22. Bourne, J. N., Sorra, K. E., Hurlburt, J. & Harris, K. M. Polyribosomes are increased in spines of CA1 dendrites 2 h after the induction of LTP in mature rat hippocampal slices. *Hippocampus* **17**, 1–4 (2007).
23. Griffiths, G. *et al.* The dynamic nature of the Golgi complex. *J. Cell Biol.* **108**, 277–297 (1989).
24. Horton, A. C. & Ehlers, M. D. Dual modes of endoplasmic reticulum-to-Golgi transport in dendrites revealed by live-cell imaging. *J. Neurosci.* **23**, 6188–6199 (2003).
25. Cui-Wang, T. *et al.* Local zones of endoplasmic reticulum complexity confine cargo in neuronal dendrites. *Cell* **148**, 309–321 (2012).
26. Horton, A. C. *et al.* Polarized secretory trafficking directs cargo for asymmetric dendrite growth and morphogenesis. *Neuron* **48**, 757–771 (2005).
27. Ye, B. *et al.* Growing dendrites and axons differ in their reliance on the secretory pathway. *Cell* **130**, 717–729 (2007).
28. Sheng, M. & Hoogenraad, C. C. The postsynaptic architecture of excitatory synapses: a more quantitative view. *Annu. Rev. Biochem.* **76**, 823–847 (2007).
29. Pielot, R. *et al.* SynProt: a database for proteins of detergent-resistant synaptic protein preparations. *Front. Synaptic Neurosci.* **4**, 1 (2012).
30. Cheng, D. *et al.* Relative and absolute quantification of postsynaptic density proteome isolated from rat forebrain and cerebellum. *Mol. Cell. Proteomics* **5**, 1158–1170 (2006).
31. Chen, X. *et al.* Mass of the postsynaptic density and enumeration of three key molecules. *Proc. Natl Acad. Sci. USA* **102**, 11551–11556 (2005).
32. Grutzendler, J., Kasthuri, N. & Gan, W. B. Long-term dendritic spine stability in the adult cortex. *Nature* **420**, 812–816 (2002).
33. Trachtenberg, J. T. *et al.* Long-term *in vivo* imaging of experience-dependent synaptic plasticity in adult cortex. *Nature* **420**, 788–794 (2002).
34. Holcman, D. & Triller, A. Modeling synaptic dynamics driven by receptor lateral diffusion. *Biophys. J.* **91**, 2405–2415 (2006).
35. Czondor, K. *et al.* Unified quantitative model of AMPA receptor trafficking at synapses. *Proc. Natl Acad. Sci. USA* **109**, 3522–3527 (2012).
36. Poon, M. M., Choi, S. H., Jamieson, C. A., Geschwind, D. H. & Martin, K. C. Identification of process-localized mRNAs from cultured rodent hippocampal neurons. *J. Neurosci.* **26**, 13390–13399 (2006).
37. Zhong, J., Zhang, T. & Bloch, L. M. Dendritic mRNAs encode diversified functionalities in hippocampal pyramidal neurons. *BMC Neurosci.* **7**, 17 (2006).
38. Lein, E. S. *et al.* Genome-wide atlas of gene expression in the adult mouse brain. *Nature* **445**, 168–176 (2007).
39. Cajigas, I. J. *et al.* The local transcriptome in the synaptic neuropil revealed by deep sequencing and high-resolution imaging. *Neuron* **74**, 453–466 (2012).
40. Kamme, F. *et al.* Single-cell microarray analysis in hippocampus CA1: demonstration and validation of cellular heterogeneity. *J. Neurosci.* **23**, 3607–3615 (2003).
41. Fiala, J. C. & Harris, K. M. *Dendrite Structure. Dendrites* (Oxford Univ. Press, 1999).
42. Shepard, P. J. *et al.* Complex and dynamic landscape of RNA polyadenylation revealed by PAS-Seq. *RNA* **17**, 761–772 (2011).
43. Derti, A. *et al.* A quantitative atlas of polyadenylation in five mammals. *Genome Res.* **22**, 1173–1183 (2012).
44. Kanehisa, M., Goto, S., Sato, Y., Furumichi, M. & Tanabe, M. KEGG for integration and interpretation of large-scale molecular data sets. *Nucleic Acids Res.* **40**, D109–D114 (2012).
45. Hanus, C. & Ehlers, M. D. Secretory outposts for the local processing of membrane cargo in neuronal dendrites. *Traffic* **9**, 1437–1445 (2008).
46. Palade, G. Intracellular aspects of the process of protein synthesis. *Science* **189**, 867 (1975).
47. Sutton, M. A. *et al.* Miniature neurotransmission stabilizes synaptic function via tonic suppression of local dendritic protein synthesis. *Cell* **125**, 785–799 (2006).
48. Mameli, M., Balland, B., Luján, R. & Lüscher, C. Rapid synthesis and synaptic insertion of GluR2 for mGluR-LTD in the ventral tegmental area. *Science* **317**, 530–533 (2007).
49. Fortin, D. A. *et al.* Brain-derived neurotrophic factor activation of CaM-kinase kinase via transient receptor potential canonical channels induces the translation and synaptic incorporation of GluA1-containing calcium-permeable AMPA receptors. *J. Neurosci.* **32**, 8127–8137 (2012).
50. Jeyifous, O. *et al.* SAP97 and CASK mediate sorting of NMDA receptors through a previously unknown secretory pathway. *Nature Neurosci.* **12**, 1011–1019 (2009).
51. Moremen, K. W., Tiemeyer, M. & Nairn, A. V. Vertebrate protein glycosylation: diversity, synthesis and function. *Nature Rev. Mol. Cell Biol.* **13**, 448–462 (2012).
52. Greger, I. H., Khatri, L. & Ziff, E. B. RNA editing at Arg607 controls AMPA receptor exit from the endoplasmic reticulum. *Neuron* **34**, 759–772 (2002).
53. Collingridge, G. L., Isaac, J. T. & Wang, Y. T. Receptor trafficking and synaptic plasticity. *Nature Rev. Neurosci.* **5**, 952–962 (2004).
54. Newpher, T. M. & Ehlers, M. D. Glutamate receptor dynamics in dendritic microdomains. *Neuron* **58**, 472–497 (2008).
55. Derr, N. D. *et al.* Tug-of-war in motor protein ensembles revealed with a programmable DNA origami scaffold. *Science* **338**, 662–665 (2012).
56. Guillaud, L., Wong, R. & Hirokawa, N. Disruption of KIF17–Mint1 interaction by CaMKII-dependent phosphorylation: a molecular model of kinesin-cargo release. *Nature Cell Biol.* **10**, 19–29 (2008).
57. Lisman, J., Yasuda, R. & Raghavachari, S. Mechanisms of CaMKII action in long-term potentiation. *Nature Rev. Neurosci.* **13**, 169–182 (2012).
58. Santamaria, F., Wils, S., De Schutter, E. & Augustine, G. J. Anomalous diffusion in Purkinje cell dendrites caused by spines. *Neuron* **52**, 635–648 (2006).
59. Bressloff, P. C. & Earnshaw, B. A. Diffusion-trapping model of receptor trafficking in dendrites. *Phys. Rev. E Stat. Nonlin. Soft Matter Phys.* **75**, 041915 (2007).
60. Petrini, E. M. *et al.* Endocytic trafficking and recycling maintain a pool of mobile surface AMPA receptors required for synaptic potentiation. *Neuron* **63**, 92–105 (2009).
61. Adesnik, H., Nicoll, R. A. & England, P. M. Photoinactivation of native AMPA receptors reveals their real-time trafficking. *Neuron* **48**, 977–985 (2005).
62. Tovar, K. R. & Westbrook, G. L. Mobile NMDA receptors at hippocampal synapses. *Neuron* **34**, 255–264 (2002).
63. Thomas, P., Mortensen, M., Hosie, A. M. & Smart, T. G. Dynamic mobility of functional $GABA_A$ receptors at inhibitory synapses. *Nature Neurosci.* **8**, 889–897 (2005).
64. Kasugai, Y. *et al.* Quantitative localisation of synaptic and extrasynaptic $GABA_A$ receptor subunits on hippocampal pyramidal cells by freeze-fracture replica immunolabelling. *Eur. J. Neurosci.* **32**, 1868–1888 (2010).
65. Luthi, A. *et al.* Hippocampal LTD expression involves a pool of AMPARs regulated by the NSF–GluR2 interaction. *Neuron* **24**, 389–399 (1999).
66. Hayashi, Y. *et al.* Driving AMPA receptors into synapses by LTP and CaMKII: requirement for GluR1 and PDZ domain interaction. *Science* **287**, 2262–2267 (2000).
67. Lu, W. *et al.* Activation of synaptic NMDA receptors induces membrane insertion of new AMPA receptors and LTP in cultured hippocampal neurons. *Neuron* **29**, 243–254 (2001).
68. Malinow, R. & Malenka, R. C. AMPA receptor trafficking and synaptic plasticity. *Annu. Rev. Neurosci.* **25**, 103–126 (2002).
69. Lai, H. C. & Jan, L. Y. The distribution and targeting of neuronal voltage-gated ion channels. *Nature Rev. Neurosci.* **7**, 548–562 (2006).
70. Harris, K. M. & Stevens, J. K. Dendritic spines of CA 1 pyramidal cells in the rat hippocampus: serial electron microscopy with reference to their biophysical characteristics. *J. Neurosci.* **9**, 2982–2997 (1989).
71. Masugi-Tokita, M. & Shigemoto, R. High-resolution quantitative visualization of glutamate and GABA receptors at central synapses. *Curr. Opin. Neurobiol.* **17**, 387–393 (2007).
72. Bourne, J. N. & Harris, K. M. Coordination of size and number of excitatory and inhibitory synapses results in a balanced structural plasticity along mature hippocampal CA1 dendrites during LTP. *Hippocampus* **21**, 354–373 (2011).
73. Gray, N. W., Weimer, R. M., Bureau, I. & Svoboda, K. Rapid redistribution of synaptic PSD-95 in the neocortex *in vivo*. *PLoS Biol.* **4**, e370 (2006).
74. El-Husseini, A. E., Schnell, E., Chetkovich, D. M., Nicoll, R. A. & Bredt, D. S. PSD-95 involvement in maturation of excitatory synapses. *Science* **290**, 1364–1368 (2000).
75. Keith, D. & El-Husseini, A. Excitation control: balancing PSD-95 function at the synapse. *Front. Mol. Neurosci.* **1**, 4 (2008).
76. Ehlers, M. D. Activity level controls postsynaptic composition and signaling via the ubiquitin-proteasome system. *Nature Neurosci.* **6**, 231–242 (2003).
77. El-Husseini Ael, D. *et al.* Synaptic strength regulated by palmitate cycling on PSD-95. *Cell* **108**, 849–863 (2002).
78. Waung, M. W., Pfeiffer, B. E., Nosyreva, E. D., Ronesi, J. A. & Huber, K. M. Rapid translation of Arc/Arg3.1 selectively mediates mGluR-dependent LTD through persistent increases in AMPAR endocytosis rate. *Neuron* **59**, 84–97 (2008).
79. Ehlers, M. D. Reinsertion or degradation of AMPA receptors determined by activity-dependent endocytic sorting. *Neuron* **28**, 511–525 (2000).
80. Lin, J. W. *et al.* Distinct molecular mechanisms and divergent endocytotic pathways of AMPA receptor internalization. *Nature Neurosci.* **3**, 1282–1290 (2000).
81. Bingol, B. & Schuman, E. M. Activity-dependent dynamics and sequestration of proteasomes in dendritic spines. *Nature* **441**, 1144–1148 (2006).
82. Patrick, G. N., Bingol, B., Weld, H. A. & Schuman, E. M. Ubiquitin-mediated proteasome activity is required for agonist-induced endocytosis of GluRs. *Curr. Biol.* **13**, 2073–2081 (2003).
83. Price, J. C., Guan, S., Burlingame, A., Prusiner, S. B. & Ghaemmaghami, S. Analysis of proteome dynamics in the mouse brain. *Proc. Natl Acad. Sci. USA* **107**, 14508–14513 (2010).
84. Cohen, L. D. *et al.* Metabolic turnover of synaptic proteins: kinetics, interdependencies and implications for synaptic maintenance. *PLoS ONE* **8**, e63191 (2013).
85. Frey, U. & Morris, R. G. Synaptic tagging and long-term potentiation. *Nature* **385**, 533–536 (1997).
86. Cleary, M. D., Meiering, C. D., Jan, E., Guymon, R. & Boothroyd, J. C. Biosynthetic labeling of RNA with uracil phosphoribosyltransferase allows cell-specific microarray analysis of mRNA synthesis and decay. *Nature Biotech.* **23**, 232–237 (2005).
87. Ngo, J. T. *et al.* Cell-selective metabolic labeling of proteins. *Nature Chem. Biol.* **5**, 715–717 (2009).
88. Ramón y Cajal, S. *Les Nouvelles Idées sur la Structure du Système Nerveux Chez l'Homme et Chez les Vertébrés* (C. Reinwald, 1894) (in French).
89. Claiborne, B. J., Amaral, D. G. & Cowan, W. M. Quantitative, three-dimensional analysis of granule cell dendrites in the rat dentate gyrus. *J. Comp. Neurol.* **302**, 206–219 (1990).
90. Andersen, P. *The Hippocampus Book* (Oxford Univ. Press, 2007).

91. Sharma, K., Fong, D. K. & Craig, A. M. Postsynaptic protein mobility in dendritic spines: long-term regulation by synaptic NMDA receptor activation. *Mol. Cell. Neurosci.* **31**, 702–712 (2006).
92. Kerr, J. M. & Blanpied, T. A. Subsynaptic AMPA receptor distribution is acutely regulated by actin-driven reorganization of the postsynaptic density. *J. Neurosci.* **32**, 658–673 (2012).
93. Ashby, M. C., Maier, S. R., Nishimune, A. & Henley, J. M. Lateral diffusion drives constitutive exchange of AMPA receptors at dendritic spines and is regulated by spine morphology. *J. Neurosci.* **26**, 7046–7055 (2006).
94. Bats, C., Groc, L. & Choquet, D. The interaction between Stargazin and PSD-95 regulates AMPA receptor surface trafficking. *Neuron* **53**, 719–734 (2007).
95. Serge, A., Fourgeaud, L., Hemar, A. & Choquet, D. Receptor activation and homer differentially control the lateral mobility of metabotropic glutamate receptor 5 in the neuronal membrane. *J. Neurosci.* **22**, 3910–3920 (2002).
96. Jacob, T. C. *et al.* Gephyrin regulates the cell surface dynamics of synaptic $GABA_A$ receptors. *J. Neurosci.* **25**, 10469–10478 (2005).
97. Renner, M., Schweizer, C., Bannai, H., Triller, A. & Levi, S. Diffusion barriers constrain receptors at synapses. *PLoS ONE* **7**, e43032 (2012).
98. Okabe, S., Urushido, T., Konno, D., Okado, H. & Sobue, K. Rapid redistribution of the postsynaptic density protein PSD-Zip45 (Homer 1c) and its differential regulation by NMDA receptors and calcium channels. *J. Neurosci.* **21**, 9561–9571 (2001).
99. Nakagawa, T., Engler, J. A. & Sheng, M. The dynamic turnover and functional roles of α-actinin in dendritic spines. *Neuropharmacology* **47**, 734–745 (2004).
100. Kuriu, T., Inoue, A., Bito, H., Sobue, K. & Okabe, S. Differential control of postsynaptic density scaffolds via actin-dependent and -independent mechanisms. *J. Neurosci.* **26**, 7693–7706 (2006).
101. Zheng, C. Y., Petralia, R. S., Wang, Y. X., Kachar, B. & Wenthold, R. J. SAP102 is a highly mobile MAGUK in spines. *J. Neurosci.* **30**, 4757–4766 (2010).
102. Nakagawa, T. *et al.* Quaternary structure, protein dynamics, and synaptic function of SAP97 controlled by L27 domain interactions. *Neuron* **44**, 453–467 (2004).
103. Tai, C. Y., Mysore, S. P., Chiu, C. & Schuman, E. M. Activity-regulated N-cadherin endocytosis. *Neuron* **54**, 771–785 (2007).
104. Star, E. N., Kwiatkowski, D. J. & Murthy, V. N. Rapid turnover of actin in dendritic spines and its regulation by activity. *Nature Neurosci.* **5**, 239–246 (2002).
105. Charrier, C. *et al.* A crosstalk between β1 and β3 integrins controls glycine receptor and gephyrin trafficking at synapses. *Nature Neurosci.* **13**, 1388–1395 (2010).
106. Pratt, J. M. *et al.* Dynamics of protein turnover, a missing dimension in proteomics. *Mol. Cell Proteom.* **1**, 579–591 (2002).
107. Ghaemmaghami, S. *et al.* Global analysis of protein expression in yeast. *Nature* **425**, 737–741 (2003).
108. Doherty, M. K., Hammond, D. E., Clague, M. J., Gaskell, S. J. & Beynon, R. J. Turnover of the human proteome: determination of protein intracellular stability by dynamic SILAC. *J. Proteome Res.* **8**, 104–112 (2009).
109. Eden, E. *et al.* Proteome half-life dynamics in living human cells. *Science* **331**, 764–768 (2011).
110. Cambridge, S. B. *et al.* Systems-wide proteomic analysis in mammalian cells reveals conserved, functional protein turnover. *J. Proteome Res.* **10**, 5275–5284 (2011).
111. Claydon, A. J., Thom, M. D., Hurst, J. L. & Beynon, R. J. Protein turnover: measurement of proteome dynamics by whole animal metabolic labelling with stable isotope labelled amino acids. *Proteomics* **12**, 1194–1206 (2012).

Acknowledgments

We are particularly grateful to L. Kochen for the data shown in figure 2 and G. Tushev for his help with data analysis. We thank I. Cajigas, S. tom Dieck and G. Tushev for their critical reading of the manuscript. We apologize to those whose work we could not cite because of space limitations. Work in the laboratory of E.M.S. is supported by the Max Planck Society, the European Research Council, DFG CRC 902 and 1080, and the DFG Cluster of Excellence for Macromolecular Complexes. C.H. is supported by a Marie Curie career integration grant.

Competing interests statement

The authors declare no competing financial interests.

FURTHER INFORMATION

KEGG: http://www.genome.jp/kegg/

ALL LINKS ARE ACTIVE IN THE ONLINE PDF